Signal, Image and Video Processing (2025) 19:928
https://doi.org/10.1007/s11760-025-04489-7

ORIGINAL PAPER

An ensemble KANs method with XAI for mitosis segmentation in histopathological images

Refik Samet[1] · Nooshin Nemati[1] · Emrah Hancer[2] · Serpil Sak[3] · Bilge Ayca Kirmizi[3]

Received: 9 February 2025 / Revised: 26 June 2025 / Accepted: 29 June 2025 / Published online: 30 July 2025
© The Author(s), under exclusive licence to Springer-Verlag London Ltd., part of Springer Nature 2025

Abstract
Mitosis in H&E-stained histopathological images is a critical prognostic marker for tumor aggressiveness, aiding in precise diagnosis and treatment planning. Accurate mitosis segmentation is essential for cancer diagnostics and therapeutic decisions. This study proposes an ensemble KANs method with XAI for mitosis segmentation. A hybrid dataset combining MIDOG21 and CCMCT is utilized, followed by enhanced stain normalization using DDPM and CD-SNMF. The ensemble KANs model incorporates XAI to improve interpretability and reliability, fostering trust in AI-assisted diagnostic tools. The proposed method achieved high performance on the hybrid dataset, with Accuracy of 0.905, Precision of 0.89, Recall of 0.88, F1-Score of 0.885, and AJI of 0.75. Experimental results demonstrate the method's effectiveness in accurately identifying mitotic cells, outperforming existing methods and enhancing digital pathology.

Keywords Histopathology images · Mitosis segmentation · Color normalization · DDPM · CD-SNMF · KANs · XAI

1 Introduction

Histopathology images, crucial for cancer diagnosis, visualize tissue morphology using stains such as Hematoxylin and Eosin (H&E). These images assist pathologists in assessing cancer type and stage, thereby guiding treatment strategies and prognosis. Among histological features, mitosis detection is a critical indicator of tumor aggressiveness, directly influencing malignancy grading and therapeutic decision-making [1]. Advances in digital pathology and image analysis have significantly improved mitosis detection, enhancing diagnostic accuracy and patient outcomes. However, several challenges persist that limit the full potential of deep learning (DL) approaches in clinical applications.

One major limitation is the size and diversity of current mitosis datasets. Public datasets such as MIDOG21 and CCMCT, while valuable, remain relatively small and lack sufficient diversity to represent the wide variability seen across different clinical environments [2]. This restriction impairs the generalization capabilities of DL models, often leading to overfitting and reduced robustness when deployed on unseen data. Expanding dataset diversity is crucial to enable models to learn a wider range of morphological patterns and staining variations, thereby improving their reliability and clinical applicability.

Another critical challenge lies in stain variability. Although H&E staining is a pathology gold standard, differences in staining protocols and scanner settings across laboratories result in substantial color variations. These inconsistencies negatively impact the performance of the DL model by introducing unwanted noise in the feature extraction [3]. Conventional stain normalization methods offer partial solutions but often fall short in preserving important histological structures. To address this, more advanced approaches that integrate Denoising Diffusion Probabilistic Models (DDPM)

✉ Nooshin Nemati
nntolakan@ankara.edu.tr

Refik Samet
samet@eng.ankara.edu.tr

Emrah Hancer
ehancer@mehmetakif.edu.tr

Serpil Sak
sak@medicine.ankara.edu.tr

Bilge Ayca Kirmizi
karabork@ankara.edu.tr

[1] Department of Computer Engineering, Ankara University, Bahcelievler, Golbası 06830, Ankara, Turkey

[2] Department of Software Engineering, Burdur Mehmet Akif Ersoy University, 15300 Burdur, Turkey

[3] Department of Pathology, Ankara University, Altındag, Ankara 6080, Ankara, Turkey

with constrained decomposition methods such as CD-SNMF [4] can enhance stain normalization, leading to more consistent and accurate feature extraction across datasets.

Despite advances in DL-based segmentation methods, achieving practical accuracy in clinical settings remains a significant hurdle. Factors such as low contrast between mitotic and non-mitotic figures, visually similar non-mitotic structures, complex tissue morphology, and imaging artifacts often result in misdetections. These limitations compromise the reliability of automated systems in real-world scenarios. Therefore, it is essential to develop segmentation models that not only perform well under controlled experimental conditions but also maintain high accuracy and robustness when faced with real-world clinical challenges.

Lastly, the lack of model transparency poses a major barrier to clinical adoption. Most state-of-the-art DL models operate as "black boxes," offering little insight into how decisions are made. This opacity undermines clinician trust, which is critical for integrating automated systems into diagnostic workflows. Explainable Artificial Intelligence (XAI) techniques, combined with inherently interpretable models such as Kolmogorov–Arnold Networks (KANs), can provide transparency by revealing the decision-making processes of segmentation models. Improving model interpretability ensures that automated predictions are not only accurate but also understandable and justifiable, thus fostering greater trust among clinicians.

In this study, we address these four critical challenges by proposing a comprehensive method with the following contributions: 1) creation of a hybrid dataset to enhance size and diversity for robust mitosis segmentation; 2) applying a stain normalization technique which combines DDPM and CD-SNMF to ensure consistent color representation; 3) proposal of an Ensemble KANs-based approach for mitosis segmentation, improving accuracy and model robustness; and 4) application of XAI techniques to explain KAN-based segmentation results, enhancing transparency and interpretability for clinical trust.

2 Related works

2.1 Mitosis datasets

The ICPR12 [5], AMIDA13 [6], and ICPR14 [7] datasets are compact and focus on breast cancer studies, while TUPAC16 [8], though larger, lacks tissue diversity. In contrast, the MIDOG21 [9] and MIDOG22 [10] datasets stand out for their size and diversity, incorporating images from various scanners, tissue types, and species. MIDOG21, however, includes challenging WSIs with variability such as out-of-focus regions and necrosis, offering unexplored negative examples. The MIDOG++ [11] dataset builds on these, enhancing WSI diversity and scope for better model evaluation. Mitosis datasets like MIDOG21 and CCMCT [12] are crucial for model development in digital pathology. MIDOG21 supports domain generalization, while CCMCT broadens representation with canine tissue annotations. Despite their benefits, the limited size and diversity of these datasets constrain model generalizability for novel clinical applications.

2.2 DL models for mitosis segmentation

Recent advances in CNN architectures have significantly influenced medical imaging by offering lightweight, high-performing, and interpretable models. For instance, Ahamed et al. have proposed several efficient DL methods that integrate feature selection, hybrid attention mechanisms, and XAI techniques, achieving outstanding results in gastrointestinal disease classification, polyp detection, and skin lesion segmentation [13, 14]. These works highlight how combining lightweight architectures, XAI, and advanced training strategies leads to models with high accuracy, fast inference times, and strong clinical interpretability—fostering broader trust and adoption in healthcare. Inspired by such progress, DL models are also at the forefront of mitosis segmentation. Topuz et al. [3] introduced CNMI-YOLO, a two-stage method combining YOLOv7 and ConvNeXt, achieving high F1-Scores across multiple datasets. Similarly, Ozturk and Akdemir [15] proposed a CNN-based semantic segmentation model tailored for mitotic events. However, these models still face challenges in generalizing across diverse staining and morphological variations. To enhance robustness, ensemble approaches like Dang et al. [16] combine multiple deep architectures, while Liu et al. [17] employed a heuristic segmentation method to improve the handling of overlapping chromosomes, boosting interpretability and segmentation accuracy. Furthermore, Bertolini et al. [18] introduced a contextualized XAI method for a multi instance learning (MIL) model trained on slide-level labels, bypassing pixel-level annotations. The methods's explanation heatmaps are validated by their agreement with pathologists' annotations and a segmentation model's predictions across datasets, including TG-GATEs. Heatmap correlations with pixel-wise annotations show alignment with tissue changes in healthy and lesion areas in TG-GATEs and other datasets.

2.3 Usage of XAI for mitosis segmentation

AI, especially deep learning (DL), plays a key role in medical image analysis, but its "black box" nature hinders acceptance in digital pathology. The importance of explainable AI (XAI) in enhancing trust, safety, and diagnostic reliability has been emphasized in prior studies, such as Longo et al. [19], which underline the need for transparency in AI decision-making.

Table 1 Main differences between previous works and the proposed method

Study	Dataset	Stain Normalization	Methods	XAI
Lijo, J. [36]	ICPR12	Color Deconvolution	U-Net+Modified VGG16	-
Topuz et al. [3]	Multiple	-	CNMI-YOLO	-
Ozturk&Akdemir [15]	Unspecified	-	CNN-based	-
Liu et al. [17]	Open datasets	-	Heuristic	Visual Feature
Bertolini et al. [18]	TG-GATEs	Macenko	Multi Instance Learning	Gradient-based
Dang et al. [16]	Unspecified	-	DNNs Ensemble	-
Proposed Method	MIDOG21+CCMCT	DDPM+CD-SNMF	Ensemble KANs	LIME

XAI allows clinicians to evaluate outputs, detect errors, and make informed corrections.

XAI methods fall into two main categories: post-hoc (explaining the model after training) and ante-hoc (inherently interpretable models). Techniques like LIME and SHAP are widely used post-hoc tools to explain deep or ensemble models, while decision trees and linear models serve as ante-hoc examples due to their transparent structures. Although rule-based approaches like Re-RX offer interpretability, they often sacrifice accuracy. In contrast, combinations such as XGBoost with SHAP provide both high predictive performance and interpretability. For example, Aravena et al. [20] successfully applied XGBoost+SHAP to identify key health variables for cancer risk prediction. Similarly, in histopathology, XAI helps clarify model decisions, building trust among clinicians [21].

Despite advancements in mitosis detection and segmentation, challenges remain due to complex mitotic morphology, low inter-class contrast, and staining variability. Although performance has improved, XAI integration in mitosis segmentation pipelines is still limited. Yet, transparency is crucial for clinical adoption, given the sensitivity of mitosis detection.

In conclusion, addressing stain normalization, developing robust segmentation models, and integrating XAI are vital steps toward improving the reliability and practical deployment of AI systems in pathology. Table 1 summarizes the key differences between previous methods and the proposed approach, emphasizing the importance of these three aspects.

2.4 KANs: Kolmogorov–Arnold networks

KANs, inspired by the Kolmogorov–Arnold representation theorem, replace traditional MLPs' fixed activation functions with learnable spline-based functions on the edges. This structural modification allows smaller KANs to match or exceed the accuracy of larger MLPs in function-fitting tasks, demonstrating faster neural scaling laws. KANs also improve interpretability due to their intuitive structure, making them suitable for small-scale AI applications. In mitosis segmentation, where mitotic figures show morphological diversity and overlap, KANs excel by providing accurate, computationally efficient, and explainable results [22].

KANs offer computational efficiency and strong performance in mitosis segmentation compared to CNNs and transformers. Unlike CNNs, which require large parameter sets, KANs utilize learnable spline-based functions to achieve high accuracy with fewer parameters, reducing overfitting and resource usage. Compared to transformer models, which are computationally intensive due to attention mechanisms, KANs enable faster training and inference through univariate function compositions. Their efficiency, interpretability, and ability to capture non-linear patterns make them well-suited for resource-constrained histopathology tasks [23].

3 Proposed approach

Fig. 1 illustrates the proposed approach, which consists of two main stages: hybrid dataset creation and preprocessing, followed by mitosis segmentation and XAI integration. First, images from the MIDOG21 and CCMCT datasets are combined, divided into patches, and normalized using CD-SNMF and DDPM methods. Then, KAN models are trained, and their outputs are fused through an ensemble model. Finally, LIME XAI is applied to provide interpretability by highlighting important regions contributing to the segmentation decisions. In the following subsections, the stages are described in detail.

3.1 Hybrid dataset creation and preprocessing

In this subsection, we first describe the creation of the hybrid dataset and patch extraction process, followed by the preprocessing techniques applied to the patches.

a) Dataset Creation: The hybrid dataset for mitosis detection is created by combining patches from the MIDOG21 and CCMCT datasets, ensuring balanced representation of human and canine tissues, as well as variations in magnifica-

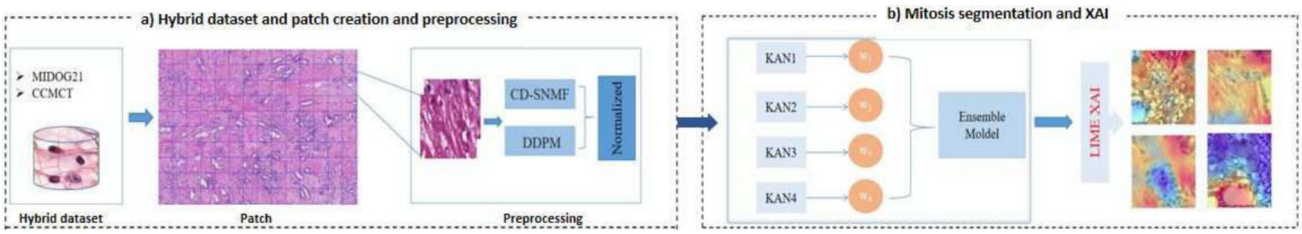


Fig. 1 The overview of the proposed approach: a) Dataset creation and preprocessing stage, (b) Mitosis segmentation with XAI stage

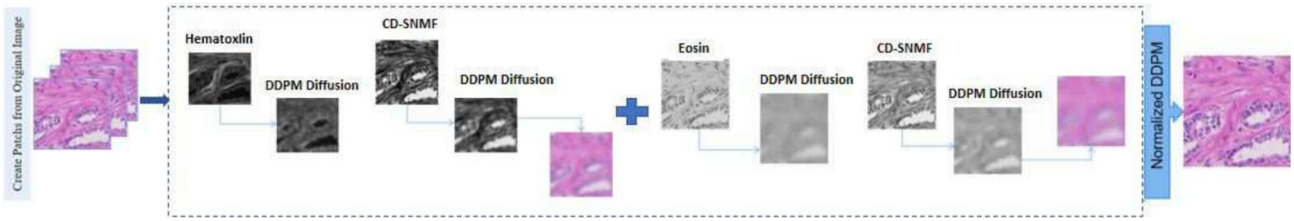


Fig. 2 The overview of the stain normalization method

tion and staining patterns. To standardize patch dimensions and resolution, 512×512 pixel patches were extracted from WSIs at $40\times$ magnification using a sliding window technique, ensuring comprehensive image coverage [24]. The extracted patches were organized into training and testing subsets, ensuring balanced representation from both datasets to prevent bias and promote generalization across species and imaging conditions. The hybrid dataset is divided into training and testing subsets with an 80% training and 20% testing split to ensure balanced representation from the MIDOG21 and CCMCT datasets. This approach addresses mitosis segmentation challenges by incorporating diverse staining patterns, tissue types, and imaging conditions, enhancing model robustness and reducing biases [25].

b) Preprocessing: Figure 2 illustrates the overall workflow of the applied stain normalization method [2], which combines CD-SNMF with a Denoising Diffusion Probabilistic Model (DDPM) to address the challenges of stain variability in histopathological images. First, CD-SNMF is applied to perform stain separation, decomposing each image into its hematoxylin and eosin components with minimal cross-talk. This step ensures that critical histopathological structures, such as nuclei and mitotic figures, are accurately isolated and preserved. Next, a DDPM is trained to model the distribution of pixel intensities associated with each stain. Through a forward diffusion process (gradually adding noise) and a learned reverse process (progressive denoising), the DDPM reconstructs images with standardized and biologically meaningful stain characteristics. This two-stage approach effectively constrains the generative behavior of the DDPM, reducing the risk of incorrect color transfers and improving stain consistency across diverse datasets.

3.2 Mitosis segmentation with ensemble KANs

This section explores ensemble technique within the KANs method to enhance the accuracy and robustness of mitosis segmentation in histopathological images. By leveraging the strengths of multiple KAN models, we aim to achieve improved segmentation performance compared to individual models. Figure 3 illustrates the structure of the KANs model.

a) KANs Layers: The KAN architecture consists of multiple layers where spline functions, $\phi_{s,p}^{(1)}(x_p)$, are applied to input features in the first layer. Subsequent layers, $\Phi_s^{(2)}(\cdot)$, $\Phi_r^{(3)}(\cdot)$, and $\Phi_q^{(4)}(\cdot)$, refine the features through additional transformations. The architecture models non-linear features of histopathological images. The general function structure of the KAN is given by:

$$f(x) = \sum_{q=1}^{2n+1} \Phi_q \left(\sum_{p=1}^{n} \varphi_{q,p}(x_p) \right) \tag{1}$$

where $x = (x_1, x_2, \ldots, x_n)$ is the input, and $\varphi_{q,p}$ and Φ_q are spline-based activation functions.

For the second and third layers, the function is as follows:

$$f(x) = \sum_{q=1}^{n_2} \Phi_q^{(3)} \left(\sum_{r=1}^{n_1} \Phi_r^{(2)} \left(\sum_{p=1}^{n} \varphi_{r,p}^{(1)}(x_p) \right) \right) \tag{2}$$

For the final output, the function is as follows:

$$f(x) = \sum_{q=1}^{n_3} \Phi_q^{(4)} \left(\sum_{r=1}^{n_2} \Phi_r^{(3)} \left(\sum_{s=1}^{n_1} \Phi_s^{(2)} \left(\sum_{p=1}^{n} \varphi_{s,p}^{(1)}(x_p) \right) \right) \right) \tag{3}$$

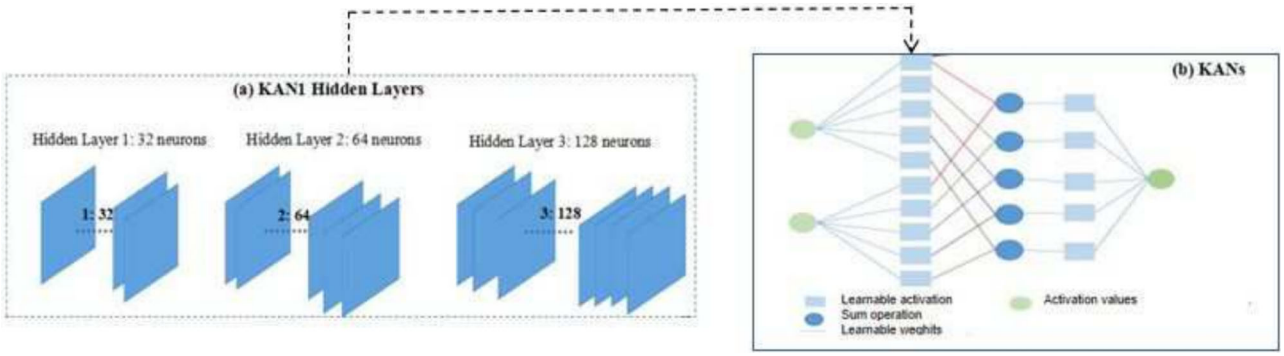


Fig. 3 (a) KAN1 hidden layers. (b) KAN architecture with hidden layers (blue rectangles) connected by learnable weights and input/output layers (green circles). Activation values of neurons are shown as blue circles

The Kolmogorov–Arnold theorem allows multivariate functions to be represented as compositions of univariate functions. The KAN network is a composition of L layers, defined as:

$$\text{KAN}(\mathbf{x}) = (\Phi_{L-1} \circ \Phi_{L-2} \circ \cdots \circ \Phi_1 \circ \Phi_0)(\mathbf{x}),$$

where $\circ$ denotes function composition, and Φ_ℓ represents the transformations in the ℓ-th layer.

b) Ensemble Model: To build a robust ensemble model, four KAN models with distinct configurations were designed to capture diverse patterns in histopathological images, influenced by staining, tissue types, and cellular characteristics. Each model featured unique neuron configurations across hidden layers:

- **KAN1:** $n_1 = 32$, $n_2 = 64$, $n_3 = 128$ for balanced performance.
- **KAN2:** $n_1 = 64$, $n_2 = 128$, $n_3 = 256$ to learn complex features.
- **KAN3:** $n_1 = 16$, $n_2 = 32$, $n_3 = 64$ for fast training and minimal overfitting.
- **KAN4:** $n_1 = 48$, $n_2 = 96$, $n_3 = 192$ for balanced capacity and generalization.

The neuron counts (n_1, n_2, n_3) impact capacity, generalization, and overfitting risks. Larger values increase complexity, while smaller values enhance training speed and generalization. KANs use fewer parameters than MLPs and CNNs, reducing overfitting while effectively capturing morphological details. By replacing linear weights with parametric splines, KANs achieve efficient training and high accuracy even with limited annotations, making them ideal for mitosis detection.

Each KAN model in the ensemble was trained on the MIDOG21, CCMCT, and hybrid datasets. The ensemble's final predictions were generated through weighted averaging, emphasizing more accurate models. Weights were computed using the following formula:

$$w_i = \frac{F1_i}{\sum_{j=1}^{4} F1_j} \tag{4}$$

where w_i is the weight for model i and $F1_i$ is its F1-score. The weighted averaging method improves the ensemble's accuracy by prioritizing stronger models and enhancing segmentation robustness.

The ensemble prediction P_{ensemble} for each pixel is computed as:

$$P_{\text{ensemble}} = w_1 \cdot p_1 + w_2 \cdot p_2 + w_3 \cdot p_3 + w_4 \cdot p_4$$

where p_i represents the probability of model i predicting mitosis. A threshold (e.g., 0.5) is applied to classify pixels. The final output is:

$$\text{Final Output} = \sum_{i=1}^{4} w_i \cdot P_i$$

3.3 Implementation of XAI

XAI comprises techniques that make AI models' decision-making processes understandable and traceable to humans. Its main goal is to clarify how and why AI makes specific predictions, allowing users to assess reliability, detect errors, and apply necessary corrections. XAI approaches are generally divided into post-hoc and ante-hoc categories. In clinical contexts—such as when an AI system suggests a cancer risk—it is crucial for clinicians to understand and justify the recommendation, making data selection and expert consultation key in defining meaningful features [26].

Among post-hoc tools, LIME stands out by segmenting input images into superpixels, perturbing them, and observing changes in predictions to infer which regions influenced the decision. Its model-agnostic nature makes it applicable even to complex models like KANs. LIME improves

Table 2 Performance of KANs and an ensemble KANs model with XAI for mitosis segmentation on three datasets

Dataset	Model	Accuracy	Precision	Recall	F1-Score	AJI
Hybrid	KAN1	0.855	0.82	0.79	0.805	0.67
	KAN2	0.882	0.86	0.845	0.852	0.71
	KAN3	0.831	0.80	0.75	0.774	0.62
	KAN4	0.870	0.85	0.82	0.835	0.68
	Ensemble	**0.905**	**0.89**	**0.88**	**0.75**	**0.75**
MIDOG21	KAN1	0.842	0.81	0.77	0.785	0.65
	KAN2	0.875	0.85	0.83	0.84	0.70
	KAN3	0.820	0.78	0.73	0.755	0.60
	KAN4	0.862	0.84	0.80	0.82	0.66
	Ensemble	**0.89**	**0.88**	**0.87**	**0.865**	**0.73**
CCMCT	KAN1	0.830	0.79	0.762	0.779	0.643
	KAN2	0.850	0.848	0.822	0.838	0.69
	KAN3	0.800	0.77	0.728	0.75	0.59
	KAN4	0.830	0.83	0.799	0.814	0.65
	Ensemble	**0.87**	**0.864**	**0.86**	**0.85**	**0.70**

transparency by visualizing key decision areas, enhancing clinical trust without affecting performance. However, its local approximation strategy, sensitivity to input changes, and tendency to oversimplify can reduce interpretability—especially in histopathology, where mitotic morphology and stain variability pose additional challenges to generating stable and meaningful explanations.

4 Results and discussion

4.1 Experiment settings

The experiment settings for the proposed ensemble method are explained as follows. Hyperparameters for the ensemble KANs model included an initial learning rate of 0.001, 100 maximum epochs, a mini-batch size of 2, L2 regularization of 0.0001, momentum of 0.9, a gradient threshold of 0.05, and the Adam optimizer. These parameters were applied to train four distinct KANs models (KAN1–KAN4) with varying neuron configurations, and their outputs were fused via weighted averaging to form the ensemble.

The evaluation metrics used in this study include Accuracy, Precision, Recall, F1-Score, and Aggregated Jaccard Index (AJI), each selected to provide a comprehensive assessment of mitosis segmentation performance. Accuracy reflects the model's overall correctness, while Precision and Recall evaluate its ability to minimize false positives and false negatives, respectively. The F1-Score balances these two measures, offering a robust indicator of detection quality. AJI, on the other hand, captures both the correct identification and precise boundary delineation of mitotic figures, which is critical given their complex morphology in histopathological images. This combination of metrics ensures a clinically meaningful evaluation aligned with the diagnostic importance of mitotic figure detection.

4.2 Ablation studies

The experiment results are respectively presented on hybrid, MIDOG21, and CCMCT datasets in Table 2 in terms of Accuracy, Precision, Recall, F1-Score, and AJI metrics. The details for KAN1-4 are provided in Section 3.2.

a) Impact of Ensemble Model: The results across the Hybrid, MIDOG21, and CCMCT datasets highlight the consistent advantage of the ensemble KAN model over its individual counterparts (KAN1–KAN4). While all KAN variants demonstrate competitive segmentation performance, the ensemble model outperforms them across all evaluation metrics. This is especially evident in the AJI, a critical metric for segmentation quality that accounts for both detection and shape alignment. The ensemble consistently achieves the highest AJI scores across all datasets, indicating superior overlap between predicted and ground truth mitotic regions. This improvement suggests that the ensemble is not only effective in identifying mitotic figures but also in delineating their boundaries with greater accuracy—an essential requirement for reliable morphological analysis in pathology. The ensemble's ability to maintain robust AJI performance even on domain-shifted datasets like MIDOG21 and CCMCT further reinforces its generalizability. Overall, these results demonstrate that ensembling KANs—particularly when combined with explainable AI techniques—significantly enhances segmentation precision and structural alignment, making it a promising approach

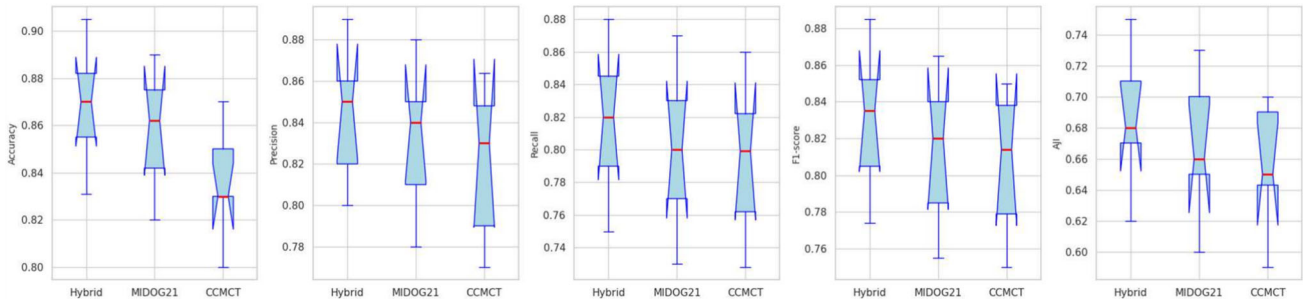


Fig. 4 Notched boxplots of performance metrics for KAN1–4 and ensemble KANs on the hybrid, MIDOG21, and CCMCT datasets (left to right: KAN1–KAN4, ensemble)



Fig. 5 Some illustrative results for LIME

Table 3 Results of the proposed method with recently introduced works

Methods	Datasets	Precision	Recall	F1-Score
Ensemble Fed CNN [27]	ICPR14	0.80	0.80	0.80
OMG-Net [28]	CCMCT	-	-	0.84
DilCasNet [29]	CCMCT	0.826	0.832	0.829
DGDMD [30]	MIDOG21	0.8307	0.8098	0.8201
ResNet50+RBF [31]	MIDOG21	0.793	0.821	0.807
FMDet [32]	MIDOG22	0.7022	0.7796	0.7389
ReCasNet [33]	CCMCT	-	-	0.832
Ensemble KANs	CCMCT	0.864	0.86	0.85
Ensemble KANs	MIDOG21	0.88	0.87	0.865
Ensemble KANs	Hybrid dataset	0.89	0.88	0.885

for trustworthy and interpretable mitosis detection in diverse histopathological contexts.

b) Impact of Hybrid Dataset: The use of the hybrid dataset plays a significant role in enhancing the generalization capability and robustness of the segmentation models. As seen in Fig. 4, compared to models trained solely on individual datasets such as MIDOG21 or CCMCT, the KANs models trained on the hybrid dataset demonstrate more balanced performance across all evaluation metrics, indicating improved adaptability to domain variations. This is particularly notable in the ensemble KANs model, which benefits from diverse data exposure during training, resulting in higher segmentation consistency. The hybrid training strategy helps mitigate the model's overfitting to specific domain characteristics by introducing inter-domain variability, which is reflected in the improved AJI across datasets. Since AJI is sensitive to both object detection and segmentation quality, its increase further validates that hybrid training enhances both localization and boundary precision. These findings suggest that incorporating a hybrid dataset during training not only strengthens the model's generalization but also provides a more reliable foundation for deployment in real-world digital pathology workflows, where staining variability and scanner differences are inevitable.

c) Impact of XAI: Some illustrative results of the LIME method are presented in Fig. 5 to improve the interpretability of the Ensemble KANs model for mitosis segmentation in histopathology images. This process generates heatmaps, as

shown in the images, where mitotic areas are highlighted in blue and less relevant areas in red. The top row of the images displays the original histopathology slides stained with H&E, showing cellular structures with mitotic figures. The bottom row presents the corresponding LIME-generated heatmaps, visually indicating the model's focus areas for mitosis detection. The study notes that LIME performed adequately, but further experiments or pathologist feedback are needed to assess its effectiveness in specific cases. LIME was chosen for its ability to provide clear, local explanations for individual predictions, which is crucial in clinical settings where transparency is vital. Its simplicity, flexibility, and ability to generate intuitive visual heatmaps make it valuable for pathologists, bridging the gap between AI decisions and human understanding. While alternatives like SHAP, Grad-CAM, or Integrated Gradients may offer deeper insights or better global interpretability, LIME's visual relevance and ease of use enhance the clinical usability of AI-assisted mitosis segmentation.

4.3 Comparisons with Recent Works

Table 3 presents a comparative analysis between the proposed Ensemble KANs method and recently introduced methods for mitosis segmentation. While recent methods such as DilCasNet, DGDMD, and ReCasNet report competitive F1-scores, the proposed Ensemble KANs consistently demonstrates superior performance across all datasets. Other methods, including FMDet and ResNet50+RBF, yield moderate results but often exhibit an imbalance between precision and recall, favoring one metric at the expense of the other. In contrast, Ensemble KANs achieve high F1-scores on CCMCT, MIDOG21, and the hybrid dataset, while maintaining a strong balance between precision and recall. This reflects the model's ability not only to detect mitotic figures accurately but also to generalize effectively across diverse staining protocols and imaging conditions. Moreover, unlike most recent studies, our evaluation includes the AJI metric a critical metric for assessing both spatial alignment and segmentation quality. The inclusion of AJI ensures a more comprehensive and fair comparison, further reinforcing the robustness and practical utility of the proposed Ensemble KANs beyond standard F1-Score-based evaluations.

5 Conclusion

This study presents an ensemble method that integrates KANs and explainable AI (XAI) for histopathological mitosis segmentation, addressing key challenges such as stain normalization, prediction accuracy, interpretability, and dataset diversity. To ensure a systematic and reproducible framework, we adopted Chou's 5-step rule [34, 35] for constructing machine learning predictors. First, a valid benchmark dataset was established by combining MIDOG21 and CCMCT, capturing diverse tissue types and staining conditions to promote generalizability. Second, image preprocessing was performed using CD-SNMF and DDPM-based stain normalization, and features were formulated using spline-based representations tailored for the KAN architecture. Third, we constructed a powerful ensemble model by integrating four complementary KAN variants, enhancing robustness through diversity. Fourth, model performance was rigorously evaluated using five-fold cross-validation on the hybrid dataset, yielding high scores across key metrics, including precision, recall, F1-Score, and AJI—highlighting both detection accuracy and spatial alignment. Finally, in line with the practical utility emphasized by Chou's framework, we plan to develop a user-friendly web server to facilitate real-world accessibility for pathologists.

To ensure the real-world applicability of the ensemble KANs model in clinical digital pathology, future work will focus on comprehensive clinical validation. This includes expanding the dataset through multi-center collaborations, conducting prospective studies with pathologists, and evaluating model outputs through blinded expert comparisons. Furthermore, the model's interpretability will be validated via XAI. These efforts aim to facilitate the model's translation into a reliable and trustworthy clinical decision-support system. Future work can focus on dataset expansion, attention mechanisms, computational optimization, and clinical validation for improved AI diagnostic tools in digital pathology.

Acknowledgements This work was supported by the Ankara University Scientific Research Projects Coordination Unit (Project ID is FCD-2022-2575).

Author Contributions R.S., N.N., and E.H. wrote the main manuscript text, prepared figures, and reviewed and revised the manuscript. S.S., B. K Resources, Investigation.

Data Availability No datasets were generated or analysed during the current study.

Declarations

Competing interests The authors declare no competing interests.

References

1. Nemati, N., Samet, R., Hancer, E., Yildirim, Z., Traore, M.: A mitosis detection and classification methodology with YOLOv5 and fuzzy classifiers. In: 9th World Congress on Electrical Engineering and Computer Systems and Sciences (EECSS'23), p. 111 (2023)
2. Samet, R., Nemati, N., Hançer, E., Sak, S., Kırmızı, B.A.: Enhanced stain normalization method for accurate mitosis detection in histopathological images. In: 9th International Conference on

Computer Science and Engineering (UBMK2024), pp. 371–376 (2024)
3. Topuz, Y., Yıldız, S., Varlı, S.: Convnext mitosis identification–you only look once (cnmi-yolo): Domain adaptive and robust mitosis identification in digital pathology. Lab. Invest. **104**(10), 102130 (2024)
4. Liu, W., Zheng, N., Lu, X.: Non-negative matrix factorization for visual coding. In: IEEE International Conference on Acoustics, Speech, and Signal Processing (ICASSP'03)., vol. 3, p. 293 (2003)
5. Ludovic, R., Daniel, R., Nicolas, L., Maria, K., Humayun, I., Jacques, K., Frédérique, C., Catherine, G., et al.: Mitosis detection in breast cancer histological images an ICPR2012 contest. J. Pathol. Inform. **4**(1), 8 (2013)
6. Veta, M., Van Diest, P.J., Willems, S.M., Wang, H., Madabhushi, A., Cruz-Roa, A., Gonzalez, F., Larsen, A.B., Vestergaard, J.S., Dahl, A.B., et al.: Assessment of algorithms for mitosis detection in breast cancer histopathology images. Med. Image Anal. **20**(1), 237–248 (2015)
7. Roux, L., Racoceanu, D., Capron, F., Calvo, J., Attieh, E., Le Naour, G., Gloaguen, A.: Mitos & atypia. Image Pervasive Access Lab (IPAL), Agency Sci., Technol. & Res. Inst. Infocom Res., Singapore, Tech. Rep 1, 1–8 (2014)
8. Veta, M., Heng, Y.J., Stathonikos, N., Bejnordi, B.E., Beca, F., Wollmann, T., Rohr, K., Shah, M.A., Wang, D., Rousson, M., et al.: Predicting breast tumor proliferation from whole-slide images: the TUPAC16 challenge. Med. Image Anal. **54**, 111–121 (2019)
9. Aubreville, M., Stathonikos, N., Donovan, T.A., Klopfleisch, R., Ammeling, J., Ganz, J., Wilm, F., Veta, M., Jabari, S., Eckstein, M., et al.: Domain generalization across tumor types, laboratories, and species—insights from the 2022 edition of the mitosis domain generalization challenge. Med. Image Anal. **94**, 103155 (2024)
10. Aubreville, M., Stathonikos, N., Bertram, C.A., Klopfleisch, R., Ter Hoeve, N., Ciompi, F., Wilm, F., Marzahl, C., Donovan, T.A., Maier, A., et al.: Mitosis domain generalization in histopathology images–the MIDOG challenge. Med. Image Anal. **84**, 102699 (2023)
11. Aubreville, M., Wilm, F., Stathonikos, N., Breininger, K., Donovan, T.A., Jabari, S., Veta, M., Ganz, J., Ammeling, J., Diest, P.J., et al.: A comprehensive multi-domain dataset for mitotic figure detection. Scientific data **10**(1), 484 (2023)
12. Bertram, C.A., Aubreville, M., Marzahl, C., Maier, A., Klopfleisch, R.: A large-scale dataset for mitotic figure assessment on whole slide images of canine cutaneous mast cell tumor. Scientific data **6**(1), 274 (2019)
13. Ahamed, M.F., Hossain, M.M., Nahiduzzaman, M., Islam, M.R., Islam, M.R., Ahsan, M., Haider, J.: A review on brain tumor segmentation based on deep learning methods with federated learning techniques. Comput. Med. Imaging Graph. **110**, 102313 (2023)
14. Ahamed, M.F., Nahiduzzaman, M., Islam, M.R., Naznine, M., Ayari, M.A., Khandakar, A., Haider, J.: Detection of various gastrointestinal tract diseases through a deep learning method with ensemble ELM and explainable AI. Expert Syst. Appl. **256**, 124908 (2024)
15. Öztürk, Ş, Akdemir, B.: A convolutional neural network model for semantic segmentation of mitotic events in microscopy images. Neural Comput. Appl. **31**, 3719–3728 (2019)
16. Dang, T., Nguyen, T.T., McCall, J., Elyan, E., Moreno-García, C.F.: Two-layer ensemble of deep learning models for medical image segmentation. Cogn. Comput. **16**, 1–20 (2024)
17. Liu, X., Wang, S., Lin, J.C.-W., Liu, S.: An algorithm for overlapping chromosome segmentation based on region selection. Neural Comput. Appl. **36**(1), 133–142 (2024)
18. Bertolini, M., Le, V.-K., Pencharz, J., Poehlmann, A., Clevert, D.-A., Villalba, S., Montanari, F.: From slides (through tiles) to pixels: an explainability framework for weakly supervised models in preclinical pathology. arXiv preprint arXiv:2302.01653 (2023)
19. Longo, L., Brcic, M., Cabitza, F., Choi, J., Confalonieri, R., Ser, J.D., Guidotti, R., Hayashi, Y., Herrera, F., Holzinger, A., Jiang, R., Khosravi, H., Lecue, F., Malgieri, G., Páez, A., Samek, W., Schneider, J., Speith, T., Stumpf, S.: Explainable artificial intelligence (XAI) 2.0: A manifesto of open challenges and interdisciplinary research directions. Inf. Fusion. **106**, 102301 (2024)
20. Selvaraju, R.R., Das, A., Vedantam, R., Cogswell, M., Parikh, D., Batra, D.: Grad-cam: Why did you say that? arXiv preprint arXiv:1611.07450 (2016)
21. Velden, B.H., Kuijf, H.J., Gilhuijs, K.G., Viergever, M.A.: Explainable artificial intelligence (xai) in deep learning-based medical image analysis. Med. Image Anal. **79**, 102470 (2022)
22. Liu, Z., Wang, Y., Vaidya, S., Ruehle, F., Halverson, J., Soljačić, M., Hou, T.Y., Tegmark, M.: Kan: Kolmogorov-arnold networks. arXiv preprint arXiv:2404.19756 (2024)
23. Khan, A., Rauf, Z., Khan, A.R., Rathore, S., Khan, S.H., Shah, N.S., Farooq, U., Asif, H., Asif, A., Zahoora, U., et al.: A recent survey of vision transformers for medical image segmentation. arXiv preprint arXiv:2312.00634 (2023)
24. Haryanto, T., Suhartanto, H., Arymurthy, A.M., Kusmardi, K.: Conditional sliding windows: An approach for handling data limitation in colorectal histopathology image classification. Inform. Med. Unlocked. **23**, 100565 (2021)
25. Aubreville, M., Wilm, F., Stathonikos, N., Breininger, K., Donovan, T.A., Jabari, S., Veta, M., Ganz, J., Ammeling, J., Diest, P.J., et al.: A comprehensive multi-domain dataset for mitotic figure detection. Scientific data **10**(1), 484 (2023)
26. Longo, L., Brcic, M., Cabitza, F., Choi, J., Confalonieri, R., Del Ser, J., Guidotti, R., Hayashi, Y., Herrera, F., Holzinger, A., et al.: Explainable artificial intelligence (xai) 2.0: A manifesto of open challenges and interdisciplinary research directions. Inf. Fusion. **106**, 102301 (2024)
27. Suresh, A.J., Nair, L.S.: Mitosis detection in breast histopathology image using ensemble features fed cnn model. In: 2023 14th International Conference on Computing Communication and Networking Technologies (ICCCNT), pp. 1–5 (2023)
28. Shen, Z., Simard, M., Brand, D., Andrei, V., Al-Khader, A., Oumlil, F., Trevers, K., Butters, T., Haefliger, S., Kara, E., et al.: A deep learning framework deploying segment anything to detect pan-cancer mitotic figures from haematoxylin and eosin-stained slides. Commun. Biol. **7**(1), 1674 (2024)
29. Li, Z., Li, X., Wu, W., Lyu, H., Tang, X., Zhou, C., Xu, F., Luo, B., Jiang, Y., Liu, X., et al.: A novel dilated contextual attention module for breast cancer mitosis cell detection. Front. Physiol. **15**, 1337554 (2024)
30. Han, J., Wang, S., Wu, L., Liu, W.: Dynamic feature extraction and histopathology domain shift alignment for mitosis detection. Image Vis. Comput. **158**, 105541 (2025)
31. Tang, Q., Cai, Y.: Deep radial basis function networks with subcategorization for mitosis detection in breast histopathology images. Med. Image Anal. **95**, 103204 (2024)
32. Wang, X., Zhang, J., Yang, S., Xiang, J., Luo, F., Wang, M., Zhang, J., Yang, W., Huang, J., Han, X.: A generalizable and robust deep learning algorithm for mitosis detection in multicenter breast histopathological images. Med. Image Anal. **84**, 102703 (2023)
33. Piansaddhayanaon, C., Santisukwongchote, S., Shuangshoti, S., Tao, Q., Sriswasdi, S., Chuangsuwanich, E.: Recasnet: Improving consistency within the two-stage mitosis detection framework. Artif. Intell. Med. **135**, 102462 (2023)
34. Khan, S., Khan, M., Iqbal, N., Hussain, T., Khan, S., Two-Level, K.: Computation model based on deep learning algorithm for identification of pirna and their functions via chou's 5-steps rule. Int. J. Pept. Res. Ther. **26**, 795–809 (2020)
35. Khan, S., Noor, S., Javed, T., Naseem, A., Aslam, F., AlQahtani, S.A., Ahmad, N.: Xgboost-enhanced ensemble model using dis-

criminative hybrid features for the prediction of sumoylation sites. BioData Mining **18**(1), 12 (2025)
36. Lijo, J.: Analysis of U-net and modified vgg16 technique for mitosis identification in histopathology images. In: 2024 International Conference on Wireless Communications Signal Processing and Networking (WiSPNET), pp. 1–8. IEEE (2024)

Publisher's Note Springer Nature remains neutral with regard to jurisdictional claims in published maps and institutional affiliations.

Springer Nature or its licensor (e.g. a society or other partner) holds exclusive rights to this article under a publishing agreement with the author(s) or other rightsholder(s); author self-archiving of the accepted manuscript version of this article is solely governed by the terms of such publishing agreement and applicable law.